

Nondestructive detections of qubits by cavity transmissions: effects of quantum correlations

L. F. Wei,^{1,2} J. S. Huang,¹ X. L. Feng,² Z. D. Wang,³ and C. H. Oh²

¹Quantum Optoelectronics Laboratory, School of Physics and Technology,
Southwest Jiaotong University, Chengdu 610031, China

²Centre for Quantum Technologies and Physics Department,
National University of Singapore, 2 Science Drive 3, Singapore 117542

³Department of Physics and Center of Theoretical and Computational Physics,
The University of Hong Kong, Pokfulam Road, Hong Kong, China

(Dated: December 21, 2018)

We propose an approach to nondestructively detect N qubits by measuring the transmissions of a dispersively-coupled cavity. By taking into account all the cavity-qubits quantum correlations (i.e., beyond the usual coarse-grained approximations), it is revealed that for an unknown normalized N -qubit state $|\psi_N\rangle = \sum_{k=0}^{2^N-1} \beta_k |k\rangle_N$, each detected peak in the cavity transmitted spectra marks one of the logic states $|k\rangle_N$ and the relative height of such a peak is related to the corresponding superposed-probability $|\beta_k|^2$. Our results are able to unambiguously account for the intriguing multi-peak structures of the spectra observed in a very recent circuit-quantum-electrodynamics experiment [Phys. Rev. A **81**, 062325 (2010)] with two superconducting qubits.

PACS numbers: 42.50.Hz, 03.67.Lx, 85.25.Cp

Introduction.— It is well-known that the readout of qubits is one of necessary steps in quantum information processing. Phenomenally, the information stored in an unknown N -qubit quantum state $|\psi_N\rangle = \sum_{k=0}^{2^N-1} \beta_k |k\rangle_N$ can be partly extracted by directly applying the standard von Neumann projective operation $\hat{P} = \sum_k |k\rangle_N \langle k|$ to the quantum register [1]. After such a projection, the register is collapsed to one of the computational basis (logic states) $\{|k\rangle_N = |\sum_{j=1}^N 2^{j-1} \alpha_j\rangle_N = \prod_{j=1}^N |\alpha_j\rangle_N, \alpha = 0, 1\}$ with a probability $|\beta'_k|^2$. This is a directly projective measurement (DPM) and the register is detected. Typically, DPM has been utilized to extract the binary quantum information stored in [2], such as trapped ions, Cooper-pair boxes, and the current-biased Josephson junctions, etc.. Essentially, due to the inevitable back actions of the measuring apparatus, the detected $|\beta'_k|^2$ is always less than its expectable value $|\beta_k|^2$. This means that the DPM is not an ideal method to extract the quantum information in an unknown quantum state [3].

Alternatively, indirectly projective measurements (IPMs) can also be utilized to achieve the measurement of the qubits, where another coupled system instead the qubits-selves is detected. Typical examples include, e.g., dc-SQUIDs for the inductively-connected Josephson flux (persistent) qubits [4], optical cavities for the containing atomic qubits [5], and Cooper-pair box for the nanomechanical resonators [6], etc.. A remarkable advantage in the IPM is that the back actions from the detected system could be minimized. If the condition $[H_N, H_I] = 0$ is satisfied (which means that the disturbance of the detector D on the qubits is negligible), then the relevant IPM further becomes a quantum nondemolition (QND) measurement [1]. Here, H_N is the Hamiltonian of the N -qubit register and H_I the interaction between it and the detector. Note that the term nondemolition does not imply that the wave function of the register fails to collapse due to the measurement [7]. In fact, for an unknown input state $|\psi_N\rangle$, after the QND measurement the N -qubit register will be automatically collapsed to one of its computational basis $|k\rangle_N$

with an *ideal* probability $|\beta_k|^2$. Thus, QND measurement is a conceptually ideal projective measurement; the successive QND measurements on the same register will give the same result.

As it can be easily detected with the current technique, driven cavity has been widely utilized to achieve the desirable IPM of the dispersively-coupling qubits. Experimentally, it is not difficult to probe the resonance frequency of a driven cavity by detecting the transmitted signals. If the qubits are dispersively coupled to the cavity mode, then the cavity is pulled by the qubits, depending on the state of the qubits. As a consequence, by detecting the shift of the central frequency of the driven cavity mode the QND measurement of the qubits can be achieved. This idea has been experimentally demonstrated by the cavity QED experiments with few qubits [8, 9], and single logic states (i.e., computational basis) of the atomic and superconducting qubits had been experimentally distinguished. Next challenge is to completely characterize an unknown N -qubit state $|\psi_N\rangle$ by nondestructively measuring an arbitrary superposition of the single logic states with ideal precisions.

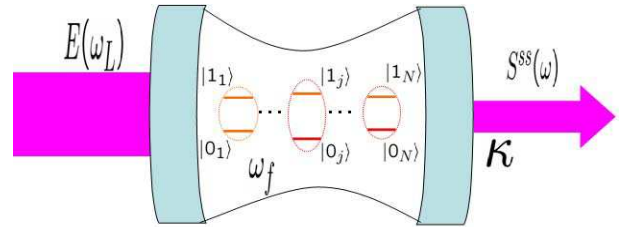


FIG. 1: (Color online) QND measurements of N qubits (with two levels: $\{|0_j\rangle, |1_j\rangle\}, j = 1, \dots, N$) by measuring the steady-state transmitted spectra $S_N^{ss}(\omega_L)$ of the dispersively-coupled cavity (with frequency ω_f and decay rate κ) driven by a frequency-controllable external field $E(\omega_L)$.

Considering the practically-existing dissipation of the detector (i.e., cavity) and also the statistical quantum correla-

tions between it and the N -qubit quantum register, in this letter we show that an unknown quantum state $|\psi_N\rangle$ can be effectively nondestructively detected by the realistic QND measurements. Immediately, our proposal can be utilized to explain well the detected multi-peak structure in the most recent circuit-quantum-electrodynamics (circuit-QED) experiment [12], where the input states of the qubits could be various superpositions of all the possible logic states.

Generic model.—The system proposed to nondestructively detect an N -qubit state is schematized in Fig. 1, wherein N non-interacting qubits are dispersively coupled to a driven cavity. Certainly, the preparation of the initial state of the qubits and detection of the driven cavity are repeatable. Without loss of generality, we assume that, the coupling strength g_j and the detuning $\Delta_j = |\omega_f - \omega_j|$ between the j th qubit and the cavity, and the detuning $\Delta_{ij} = |\omega_i - \omega_j|$ between the i th and j th qubits satisfy the condition

$$0 < \frac{g_j}{\Delta_j}, \frac{g_i g_j}{\Delta_i \Delta_{ij}}, \frac{g_i g_j}{\Delta_j \Delta_{ij}} \ll 1, \quad i \neq j = 1, 2, \dots, N. \quad (1)$$

This is to realize the dispersive interactions between the qubits and cavity, and to assure that the i th and j th qubits are decoupled effectively from each other. Also, the decay rates $\{\gamma_j\}$ of the qubits should be significantly less than that of the cavity, κ , to ensure that the detected state of the qubits has sufficiently-long lifetime. In fact, all the conditions listed above are practically satisfied in the current typical circuit-QED systems [9].

Under the rotating-wave approximation and in a framework rotating at a frequency ω_L , the process for nondestructively measuring the unknown N -qubit state could be described by the following master equation

$$\begin{aligned} \dot{\rho}_N &= -i[H_N, \rho_N] + \frac{\kappa}{2}(2\hat{a}\rho_N\hat{a}^\dagger - \hat{a}^\dagger\hat{a}\rho_N - \rho_N\hat{a}^\dagger\hat{a}), \\ H_N &= \delta\hat{a}^\dagger\hat{a} + \frac{1}{2}\sum_{j=1}^N\tilde{\omega}_j\sigma_j^z - \hat{a}^\dagger\hat{a}\sum_{j=1}^N\Gamma_j\sigma_j^z + \epsilon(\hat{a}^\dagger + \hat{a}), \end{aligned} \quad (2)$$

with $\Gamma_j = g_j^2/\Delta_j$ and ϵ being the effective strength of the driving. Also, $\tilde{\omega}_j = \omega_j - \Gamma_j$ is the renormalized transition frequency of the j th qubit, and $\delta = \omega_f - \omega_L$ is the detuning between the driving field and the cavity. Given that the dissipation of the qubits is negligible, the expectable values of all the related qubit-operators, i.e., σ_j^z , $\sigma_j^z\sigma_k^z$ ($j \neq k$), and the N -body ones $\prod_{j=1}^N\sigma_j^z$ are kept unchanged. Our central task is to calculate the steady-state transmitted strength $S_N^{ss}(\omega_L)$ of the driven cavity. This quantity is essentially proportionate to the number of the steady-state photons in the cavity, i.e., $S_N^{ss} = \langle\hat{a}^\dagger\hat{a}\rangle_N^{ss}/\epsilon^2$, which is determined by the following dynamical equation

$$\frac{d\langle\hat{a}^\dagger\hat{a}\rangle_N}{dt} = -\kappa\langle\hat{a}^\dagger\hat{a}\rangle_N - 2\epsilon\text{Im}\langle\hat{a}\rangle_N. \quad (3)$$

Here, $\langle\hat{a}\rangle_N = \text{Tr}(\hat{a}\rho_N)$ is further determined by

$$\frac{d\langle\hat{a}\rangle_N}{dt} = \left(-i\delta - \frac{\kappa}{2}\right)\langle\hat{a}\rangle_N + i\sum_{j=1}^N\Gamma_j\langle\sigma_j^z\hat{a}\rangle_N - i\epsilon. \quad (4)$$

Neglecting all the statistical quantum correlations between the cavity and qubits, i.e., under the usual coarse-grained (or mean-field) approximation (CGA), we simply have $\langle\sigma_j^z\hat{a}\rangle_N \approx \langle\sigma_j^z(0)\rangle_N\langle\hat{a}\rangle_N$. Then, by finding the steady-state solutions to the Eqs. (3-4), one can easily obtain an approximate transmitted spectrum:

$$\tilde{S}_N^{ss}(\omega_L) = \left\{[\omega_L - (\omega_f - \Delta\tilde{\omega}_N)]^2 + \left(\frac{\kappa}{2}\right)^2\right\}^{-1}, \quad (5)$$

with $\Delta\tilde{\omega}_N = \sum_{j=1}^N\Gamma_j\langle\sigma_j^z(0)\rangle_N$. This indicates that, compared to the spectrum for the empty cavity (EMC) transmission, the qubits only shift the central frequency with a quantity $\Delta\tilde{\omega}_N$ and the single-peak shape is unchanged. However, the above CGA is unnecessary and the two-body cavity-qubits correlation functions $\langle\sigma_j^z\hat{a}\rangle_N$ can be further determined by solving the following dynamical equation

$$\frac{d\langle\sigma_j^z\hat{a}\rangle_N}{dt} = \left(-i\delta - \frac{\kappa}{2}\right)\langle\sigma_j^z\hat{a}\rangle_N - i\epsilon\langle\sigma_j^z\rangle_N + i\sum_{l=1}^N\Gamma_l\langle\sigma_l^z\sigma_j^z\hat{a}\rangle_N. \quad (6)$$

Note that the three-body cavity-qubits correlations $\langle\sigma_j^z\sigma_l^z\hat{a}\rangle_N$, introduced above, is related further to the four-body cavity-qubits correlations: $\langle\sigma_j^z\sigma_l^z\sigma_m^z\hat{a}\rangle_N$, $m = 1, 2, \dots, N$, etc.. Generally, the k -body cavity-qubits correlations are related further to the $(k+1)$ -body cavity-qubits correlations (i.e., k qubits correlate simultaneously to the cavity), and thus a series of dynamical equations for these correlations will be induced. Fortunately, due to the fact that $\sigma_l^z\sigma_m^z = 1$ for $l = m$, these equation-chains will be automatically cut off and ended at the $(N+1)$ -body cavity-qubits correlations. Finally, all the interested statistical quantum correlations in these equations can be exactly calculated, and consequently the transmitted spectra can be obtained beyond the usual CGAs. It is emphasized that the spectral distribution $S_N^{ss}(\omega_L)$ including all the cavity-qubits quantum correlations may reveal 2^N peaks for an N -qubit state superposed by 2^N logic states. If the detected state is just one of the logic states (not their superposition), then $S_N^{ss}(\omega_L)$ reduces to $\tilde{S}_N^{ss}(\omega_L)$ (with a single-peak structure) and the cavity-qubits quantum correlation vanishes.

Demonstrations with experimentally-existing circuit-QED systems.—Our generic proposal derived above could be specifically demonstrated with various experimental cavity-qubits systems, typically the circuit-QED one [9, 14]. In this system, the cavity is formed by a coplanar waveguide (of the length at the order of millimeters) and the qubits are generated by the Cooper-pair boxes (CPBs) with controllable Josephson energies. At a sufficiently low temperature (e.g., ≤ 20 mK), the coplanar waveguide works as an ideal superconducting transmission line resonator (i.e., cavity). Experimentally [10], the decay rate (e.g., $\kappa = 2\pi \times 1.69\text{MHz}$) of the cavity is about ten times larger than that of the CBP-qubit (e.g., $\gamma = 2\pi \times 0.19\text{MHz}$) [11]. Also, by adjusting the external biases, the CPB-qubits could be either coupled to or decoupled from the resonator, and the required initial state preparation and detection can be robustly repeated. For the EMC case, the steady-state solutions to Eqs. (3-4) can be easily obtained and the transmission spectrum reads

$S_0^{ss}(\omega_L) = [(\omega_L - \omega_f)^2 + (\kappa/2)^2]^{-1}$. Obviously, this is a well-known Lorentzian lineshape centered at ω_f , with the half-width κ .

For one qubit case with $N = 1$, the steady-state transmission spectrum of the cavity is expressed as

$$S_1^{ss}(\omega_L) = \frac{(\omega_L - \omega_f)^2 - 2(\omega_L - \omega_f)\Gamma_1\langle\sigma_1^z(0)\rangle_1 + \Lambda_1}{[(\omega_L - \omega_f)^2 - \Lambda_1^2] + [\kappa(\omega_L - \omega_f)]^2}, \quad (7)$$

with $\Lambda_1 = \Gamma_1^2 + \kappa^2$ and $\langle\sigma_1^z(0)\rangle_1 = 2|\beta_1|^2 - 1$ for the unknown qubit state $|\psi_1\rangle$. This is evidently different from the $\tilde{S}_1^{ss}(\omega_L)$ derived under the usual CGA. Obviously, the spectrum function $S_1^{ss}(\omega_L)$ predicates that two transmitted peaks could be found in the spectrum.

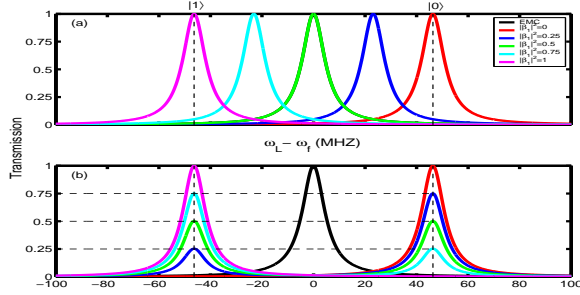


FIG. 2: (Color online) Spectral distributions $\tilde{S}_1^{ss}(\omega_L)$ (a) and $S_1^{ss}(\omega_L)$ (b) of the cavity with a single qubit prepared at the state $|\psi\rangle_1 = \beta_0|0\rangle_1 + \beta_1|1\rangle_1$, typically for $|\beta_1|^2 = 0, 0.25, 0.5, 0.75$, and 1, respectively. In contrast, transmission spectrum of the empty cavity (EMC) $S_0^{ss}(\omega_L)$ is also shown by the black line.

Specifically, using the parameters in the experimental circuit-QED with one CPB-qubit [10]: $(\omega_f, \omega_0, \kappa, g) = 2\pi \times (6444.2, 4009, 1.69, 134)$ MHz, we plot respectively the spectra $\tilde{S}_1^{ss}(\omega_L)$ and $S_1^{ss}(\omega_L)$ in Figs. 2(a) and 2(b) typically for $|\beta_1|^2 = 0, 0.25, 0.5, 0.75$, and 1, respectively. For contrast, the spectrum of the empty cavity (black line) is also plotted in the figures. We make two remarks. Firstly, if the qubit is at one of their logic states (i.e., either $|0\rangle_1$ or $|1\rangle_1$), then $\tilde{S}_1^{ss}(\omega_L)$ and $S_1^{ss}(\omega_L)$ give the same single-peak distribution, which has been experimentally demonstrated [9]. Secondly, if the qubit is prepared beforehand at the superposition of its two logic states, then $\tilde{S}_1^{ss}(\omega_L)$ shows still the single-peak structure (when $|\beta_1| = 0.5$, $\tilde{S}_1^{ss}(\omega_L)$ superposes the $S_0^{ss}(\omega_L)$) but $S_1^{ss}(\omega_L)$ predicts two peaks: the locations of the central frequencies are unchanged, but their relative heights equal respectively to the superposed probabilities of the two logic states. Therefore, $S_1^{ss}(\omega_L)$ (rather than $\tilde{S}_1^{ss}(\omega_L)$) provides the messages of all the diagonal elements of the density matrix ρ_1 . These predictions should be easily verified with the current experimental technique [9], once the qubit is input at a selected superposition state.

Similarly, for $N = 2$ case [12–14] the steady-state transmitted spectrum can still be analytically obtained:

$$S_2^{ss}(\omega_L) = -\frac{2(AC + BD)}{\kappa(A^2 + B^2)}, \quad (8)$$

with $A = (\Gamma_1^2 - \Gamma_2^2)^2 + 2[\frac{\kappa^2}{4} - (\omega_L - \omega_f)^2] \sum_{j=1}^2 \Gamma_j^2 + [\frac{\kappa^2}{4} - (\omega_L - \omega_f)^2]^2 - \kappa^2(\omega_L - \omega_f)^2$, $B = -2\kappa(\omega_L - \omega_f)[\sum_{j=1}^2 \Gamma_j^2 + \frac{\kappa^2}{4} - (\omega_L - \omega_f)^2]$, $C = \kappa\langle\sigma_1^z(0)\sigma_2^z(0)\rangle_2\Gamma_1\Gamma_2 - \kappa(\omega_L - \omega_f) \sum_{j=1}^2 \langle\sigma_j^z(0)\rangle_2\Gamma_j + \frac{\kappa}{2}[3(\omega_L - \omega_f)^2 - \frac{\kappa^2}{4} - \sum_{j=1}^2 \Gamma_j^2]$, and $D = -2\langle\sigma_1^z(0)\sigma_2^z(0)\rangle_2(\omega_L - \omega_f)\Gamma_1\Gamma_2 - \sum_{j=1}^2 \langle\sigma_j^z(0)\rangle_2\Gamma_j[\Gamma_j^2 - \Gamma_{j'}^2 + \frac{\kappa^2}{4} - (\omega_L - \omega_f)^2] + (\omega_L - \omega_f)[\sum_{j=1}^2 \Gamma_j^2 + \frac{3\kappa^2}{4} - (\omega_L - \omega_f)^2]$, $j \neq j' = 1, 2$, respectively. It is seen that, the spectral distribution $\tilde{S}_2^{ss}(\omega_L)$ may reveal four peaks, but $\tilde{S}_2^{ss}(\omega_L)$ always shows one-peak structure. Below, we show that this prediction can immediately be verified by the detected multi-peak structure of the cavity transmissions in the most recent circuit QED experiment with two qubits [12].

Experimental data shown in Fig. 1 of Ref. [12] reveal clearly one-, two-, and four peaks transmitted spectra, corresponding respectively to four different two-qubit states. The strengths of the homodyne voltage-signals detected there are just proportional to the steady-state mean photons calculated above. Physically, Hamiltonian (1) in Ref. [12] also implies that, if the two-qubit is prepared only at one of four logic states, then only one peak should be detected. While, the detected two (two, four)-peak structure means that the two-qubit is practically prepared at the superposition of the two (two, four) logic states, since there are two (two, four) possible frequency-shifts of the cavity pulled by the different logic states of the qubits. Based on such a logic and using the same experimental parameters [12, 13]: $(\omega_f = \omega_c, \Gamma_1 = \chi^L, \Gamma_2 = \chi^R, \kappa) = 2\pi \times (6.806, 0.013, 0.004, 0.001)$ GHz, we plot the spectral function $\tilde{S}_2^{ss}(\omega_L)$ calculated above in Fig. 3 for the selected two-qubit state $|\psi_2\rangle$ with: $(|\beta_0|^2, |\beta_1|^2, |\beta_2|^2, |\beta_3|^2) = (1, 0, 0, 0)$ (black line), $(0.34, 0.66, 0, 0)$ (blue line), $(0.47, 0, 0.53, 0)$ (red line), and $(0.2, 0.2, 0.26, 0.34)$ (pink line), respectively. Clearly, our simulations agree well with the experimental data shown in the Fig. 1 of Ref. [12] on both the locations of the peaks and their relative heights: (i) Our black line shows a single peak, which is consistent with the detected circles there. This implies that in this case the two-qubit was initialized at its ground state $|00\rangle = |0\rangle_2$. (ii) The two-peak structure indicated in the simulated red line is significantly consistent with those in the detected triangles there. Thus, the two-qubit in this case was prepared probably at a superposed state $\beta_0|0\rangle_2 + \beta_2|2\rangle_2$ with $|\beta_0|^2 \approx 0.47$ and $|\beta_2|^2 \approx 0.53$. (iii) The blue line simulated in Fig. 3 here directly corresponds to the squares demonstrated experimentally, just the relative heights detected are slightly higher than those of the simulated ones. This is because that there are some overlaps between these two detected transmitted peaks (due to the experimental imprecisions). Similar situations exist also in the detected diamonds. Apparently, these deviations are not intrinsic. Therefore, one can conjecture that for the squares the detected two-qubit was prepared at the superposition of the logic states $|0\rangle_2$ and $|1\rangle_2$, while for the diamonds the two-qubit should be prepared beforehand at the superposition of all the four possible logic states with the relevant probabilities.

Generally, one could presume that the QND measurements

of an arbitrary N -qubit state $|\psi_N\rangle$ could be achieved by analyzing the transmission spectra of the their dispersively-coupled cavity. From the locations of the central frequencies of the detected peaks, one can determine which logic states $\{|k\rangle_N\}$ are superposed; and from the relative heights of the corresponding peaks, one can determine the superposed probabilities $\{|\beta_k|^2\}$. Therefore, all the diagonal elements of the density matrix $\rho_N = |\psi_N\rangle\langle\psi_N|$ can be directly read out by these QND spectral detections.

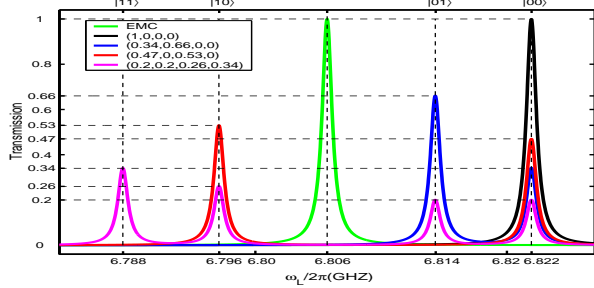


FIG. 3: (Color online) Transmission spectra of the driven circuit QED with two qubits prepared at the state $|\psi_2\rangle = \sum_{k=0}^3 \beta_k |k\rangle_2$ typically with $(|\beta_0|^2, |\beta_1|^2, |\beta_2|^2, |\beta_3|^2) = (|\beta_0|^2, |\beta_1|^2, |\beta_2|^2, |\beta_3|^2) = (1, 0, 0, 0)$ (black line), $(0.34, 0.66, 0, 0)$ (blue line), $(0.47, 0, 0.53, 0)$ (red line), and $(0.2, 0.2, 0.26, 0.34)$ (pink line), respectively. These simulations agree well with the experimental measurements shown by the Fig. 1 in Ref. [12]. Here, all the spectral lines are normalized to unity, i.e., the sum of the relative heights of the peaks in each line is unity.

Discussions and Conclusions.—The spectral QND measurements of the N qubits proposed here are implemented by measuring the transmitted spectra of their dispersively-coupled cavity. These are the IPMs of the qubits, and thus the detected results are still the so-called ensemble averages. By the analysis with simple one- and two-qubit examples, we have quantitatively shown that the our generic predictions are experimentally verifiable.

Physically, the multi-peak structure originates from such an argument: if the N -qubit register is prepared at the superposition of $M(\leq 2^N - 1)$ logic states, then the cavity could be pulled by M forms and thus there are M possible shifts of the cavity resonance frequency. Therefore, the detected cavity transmitted spectrum will reveal M peaks; the superposed probability of one of the logic state determines the weight for pulling the cavity and thus the relative height of the corresponding transmitted peak.

Immediately, our spectral QND measurements provide a relatively-simple tomographic technique to reconstruct the density matrix ρ_N . Given only one kind of the proposed measurements can directly determine all the diagonal elements in ρ_N , non-diagonal elements in the matrix ρ_N could also be determined by other spectral QND measurements by transferring them to the diagonal locations via designable unitary operations. For example, 6 kinds linearly-independent spectral QND measurements are sufficient to tomographically reconstruct the 4×4 density matrix of an unknown two-qubit state $|\psi_2\rangle$. This is essentially simpler than the usual tomographic technique based on many (i.e., fifteen) kinds of DPMs [15].

Remarkably, our proposal is a theory beyond the usual CGA and thus the statistical quantum correlations between the cavity and qubits are important, although their interactions are dispersive (i.e., far from the resonances). By specifically solving the dynamical equation of the cavity-qubit correlations for $N = 1$ case, one can prove that the lifetime of the qubit-cavity quantum correlation is sufficiently long, e.g., it is almost the same as that of the cavity-self. Therefore, the effects of the cavity-qubit correlations should be taken into account.

Acknowledgments

This work was supported in part by the National Science Foundation grant No. 10874142, 90921010, and the National Fundamental Research Program of China through Grant No. 2010CB923104, and A*STAR of Singapore under research grant No. WBS: R-144-000-189-305. One of us (Wei) thanks also Drs. Y. Yu and M.W. Wu for useful comments.

- [1] V. B. Braginsky and F. Ya. Khalili, *Quantum Measurement* (Cambridge University Press, 1992); Rev. Mod. Phys. **68**, 1(1996).
- [2] See, e.g., D. Leibfried *et al.*, Rev. Mod. Phys. **75**, 281 (2003); G. Johansson *et al.*, J. Phys.: Cond. Mat. **18** S901 (2006); K.P. Cooper *et al.*, Phys. Rev. Lett. **93**, 180401 (2004).
- [3] T. C. Ralph *et al.*, Phys. Rev. A **73**, 012113 (2006); A. N. Korotkov, Phys. Rev. B **78**, 174512 (2008).
- [4] T. Picot *et al.*, Phys. Rev. Lett. **105**, 040506 (2010); A. Lupascu, Nature Phys. **3**, 119 (2007).
- [5] J. M. Raimond *et al.*, Rev. Mod. Phys. **73**, 565 (2001).
- [6] M. D. LaHaye *et al.*, Nature **459**, 960 (2009); L. F. Wei *et al.*, Phys. Rev. Lett. **97**, 237201 (2006).
- [7] D. Wahyu Utami and A. A. Clerk, Phys. Rev. A **78**, 042323 (2008); L. Chirulli and G. Burkard, Phys. Rev. B **80**, 184509 (2009).
- [8] H. J. Kimble, in *Cavity Quantum Electrodynamics*, edited by P.

- Bermann (Academic Press, San Diego, 1994); T. Fischer *et al.*, Phys. Rev. Lett. **88**, 163002 (2002).
- [9] A. Wallraff *et al.*, Nature **431**, 162(2004); Phys. Rev. Lett. **95**, 060501 (2005); A. Blais *et al.*, Phys. Rev. A **75**, 032329 (2007).
- [10] R. Bianchetti *et al.*, Phys. Rev. A **80**, 043840(2009).
- [11] Taking into account the dissipation $\{\gamma_j\}$ and and dephasing $\{\gamma_{\phi,j}\}$ of the qubits, the proposed spectral QND measurements will be described by a more generic master equation: $\dot{\rho}_N = -i[H_N, \rho_N] + \kappa \mathcal{D}[a]\rho_N + \sum_j \gamma_j \mathcal{D}[\sigma_{-j}]\rho_N + \sum_j \frac{\gamma_{\phi,j}}{2} \mathcal{D}[\sigma_{z_j}]\rho_N$, with the dissipation superoperator $\mathcal{D}[A]\rho_N = A\rho_N A^\dagger - A^\dagger A\rho_N/2 - \rho_N A^\dagger A/2$. Thus, the expectable values of the qubit operators should not be theoretically unchanged during the desirable QND measurements. For example, one can find the decay: $\langle\sigma_{z_j}(t)\rangle = \exp(-\gamma_{1,j}t)\langle\sigma_{z_j}(0)\rangle$. However, compared with the sufficiently short detecting time $T_e \approx 40$ ns [10], the decay/dissipation of the qubit is significantly small, e.g.,

- $\gamma_{1,1} \sim 2\pi \times 0.02$ MHz [9], and thus is really negligible (i.e., $\exp(-\gamma_{1,j}t) \sim 1$).
- [12] J.M. Chow *et al*, Phys. Rev. A **81**, 062325 (2010).
 [13] L. DiCarlo *et al*, Nature **460**, 240 (2009).
 [14] S. Filipp *et. al.*, Phys. Rev. Lett. **102**, 200402 (2009).
 [15] C. F. Roos *et. al.*, Phys. Rev. Lett. **92**, 220402 (2004); Y.-x, Liu, L. F. Wei, and F. Nori, Phys. Rev. B **72**, 014547(2005).